Construction and Building Materials 182 (2018) 646–656

Contents lists available at ScienceDirect

Construction and Building Materials

journal homepage: www.elsevier.com/locate/conbuildmat

Development of new pH-adjusted fluorogypsum-cement-fly ash blends: Preliminary investigation of strength and durability properties

Yasser Bigdeli [a], Michele Barbato [a,*], Maria Teresa Gutierrez-Wing [b], Charles D. Lofton [a], Kelly A. Rusch [c], Jongwon Jung [d], Jungyeon Jang [a]

[a] Department of Civil and Environmental Engineering, Louisiana State University, Baton Rouge, LA 70803, USA
[b] Sea Grant/AGGRC, School of Renewable Natural Resources, Louisiana State University, Baton Rouge, LA 70820, USA
[c] Vice presidency of Research and Creative Activity and Department of Civil and Environmental Engineering, North Dakota State University, Fargo, ND 58105, USA
[d] School of Civil Engineering, Chungbuk National University, Cheongju-si, Chungbuk 28644, South Korea

HIGHLIGHTS

- New fluorogypsum-fly ash-Portland cement blend for outdoor/underwater construction.
- Preliminary investigation of strength and durability properties.
- Investigation of effects of different compositions.
- Other relevant properties investigated for a promising composition.
- Identified promising compositions for outdoor/underwater applications.

ARTICLE INFO

Article history:
Received 6 September 2017
Received in revised form 26 May 2018
Accepted 9 June 2018

Keywords:
Fluorogypsum
Fly ash
Portland cement
Compressive strength
Modulus of elasticity
Poisson's ratio
Volumetric expansion
Response surface model

ABSTRACT

This paper develops a new low-cost construction material made of pH-adjusted fluorogypsum, class C fly ash, and type II Portland cement. The proposed fluorogypsum-based blend is durable in water and has a lower weight and lower cost than ordinary concrete. A preliminary investigation of strength and durability properties of this new construction material is also presented. A series of compressive strength tests and volumetric expansion measurements were conducted on specimens after 28 days of curing. The experimental results were used to develop response surface models. These models can be used to predict accurately compressive strength and volumetric expansion as functions of the relative content, in dry weight, of different components. The response surface models were employed to determine ranges of dry components of the system with sufficient strength and limited volumetric expansion. A composition with 62% pH-adjusted fluorogypsum, 35% fly ash, and 3% Portland cement was selected based on strength and volumetric expansion properties to conduct additional experimental studies to quantify its modulus of elasticity, Poisson's ratio, setting times, density, void contents, and curing time effects on strength and volumetric expansion. The investigation results suggest that the proposed fluorogypsum-based blend is a promising low-cost concrete-like material for use in outdoor and underwater construction applications.

1. Introduction

Millions of tons of solid by-product materials are generated by industrial processes throughout the world every year and are accumulated over time in landfills. This large accumulation of industrial by-products represents a significant environmental hazard, produces substantial costs to public organizations and private companies, and generates significant economic and social losses [1]. The use of solid industrial by-products in the construction industry has received significant attention due to the large worldwide demand of construction materials starting from the late 1970s [2–4]. In particular, the following benefits of using by-product materials in construction have been identified: (1) reduction of construction costs [5]; (2) reduction of construction carbon footprint [6,7]; (3) limitation of undesirable environmental impacts by reducing the amount of by-products introduced in the environment [8]; and (4) reduc-

* Corresponding author.
E-mail addresses: ybigde1@lsu.edu (Y. Bigdeli), mbarbato@lsu.edu (M. Barbato), mgutie5@lsu.edu (M.T. Gutierrez-Wing), clofto5@lsu.edu (C.D. Lofton), kelly.rusch@ndsu.edu (K.A. Rusch), jjung@chungbuk.ac.kr (J. Jung), jjang2@lsu.edu (J. Jang).

https://doi.org/10.1016/j.conbuildmat.2018.06.086
0950-0618/

tion of the land loss caused by the disposal of these by-product materials [8].

Among these industrial by-products, several types of gypsum materials are used for different applications in the construction industry [9]. This study focuses on the use of fluorogypsum (FG) for outdoor and underwater construction applications. FG is an acidic by-product generated during the industrial production of hydrofluoric acid (HF) from fluorspar. FG is discharged in the form of slurry into a holding pond until it becomes a solidified dry residue with low pH after water evaporation [10]. The total consumption of fluorspar in US was 601,000 metric tons in 2001; 60–65% of this consumption (i.e., 376,000 metric tons) was used to produce HF [11]. Based on the chemical reaction for HF production, i.e.,

$$CaF_2 + H_2SO_4 \rightarrow 2HF + CaSO_4 \quad (1)$$

the production of FG in 2001 can be estimated as about 660,000 metric tons [12]. The 2015 production capacity of FG in Louisiana alone was about 360,000 metric tons (G. Mitchell, Brown Industries, personal communication, 2015). Before use, the dry FG is removed from the holding pond, mixed with 2%–5% of alkali materials such as lime or circulating fluidized bed combustion (CFBC) ash [13], crushed and screened to obtain a pH-adjusted, well-graded sandy silt material with gravel size grains [10], referred to as pH-adjusted FG hereinafter. The pH-adjusted FG has pH $\approx$ 7 due to the reaction of the alkali materials with the residual sulfuric acid in the slurry FG.

Blends of pH-adjusted FG with other cementitious materials (e.g., Portland cement, fly ash, lime, and/or ground granulated blast furnace slag) have recently attracted the attention of researchers for use as pavement base materials [14–16], as a non-structural plaster for indoor applications, and as a structural material for outdoor applications [17]. However, to the knowledge of the authors, the use of FG-based blends in underwater applications has not been considered in the literature, most likely due to their relatively long setting time [17] and to the durability issues caused by the moderate solubility of gypsum materials in water, which can dramatically decrease the mechanical strength of gypsum-based blends [18]. The research presented in this manuscript is the first preliminary investigation on the strength and durability properties of pH-adjusted FG-cement-fly ash blends in order to determine the feasibility of their usage for outdoor and underwater applications.

2. Research objective, needs, and relevance

The objective of this paper is to develop a low-cost FG-based blend that can be used as a construction material for outdoor and underwater applications. The proposed blend is made of: (1) pH-adjusted FG, (2) class C fly ash (FA), and (3) type II Portland cement (PC). In this study, the pH-adjusted FG material is utilized as provided by the producer, i.e., it already contains 2%–5% CFBC ash and it is not further processed to modify and/or improve its characteristics before its use as a component of the FG-based blends. As such, the resulting blend contains grains of a 2 cm maximum diameter. These grains of pH-adjusted FG effectively behave as coarse aggregate and the resulting FG-based blend can be considered a concrete system, in which the binder consists of the mix of fine pH-adjusted FG, FA, and PC. It is also noteworthy that the investigation presented in this paper aims to develop an FG-based blend that can be used as a direct low-cost substitute for Portland cement concrete and/or crushed limestone in a variety of outdoor and underwater applications.

Utilization of FG-based blends can potentially present some important advantages over the usage of Portland cement concrete in outdoor construction applications and of limestone in road base and underwater applications, e.g.: (1) lower unit weight of the blend (with values contained between 70% and 92% of the concrete unit weight, see [17]) and, thus, lighter structures; (2) lower cost of production, e.g., FG-based blends contain only small amounts of Portland cement (i.e., less than 10% in weight of the dry components) and have a considerably lower cost than ordinary concrete [21]; (3) lower carbon footprint, e.g., due to the lower amounts of Portland cement in FG-based blends than in ordinary concrete; and (4) wider availability of pH-adjusted FG in US coastal regions where aggregate for concrete or limestone is not readily available [22,23]. However, additional understanding of the physical, chemical, and mechanical behavior of FG-based blends is needed to develop a material that can be reliably used for outdoor and underwater construction applications. This understanding is a crucial prerequisite to determine the feasibility of FG-based blends, identify additional research needs, and support future development of this type of material.

In this work, strength and durability properties of FG-based blends made of different amounts of pH-adjusted FG, PC, and FA are investigated. Two response surface models (RSMs) are developed for the prediction of compressive strength and volumetric expansion for different FG-based compositions after 28 days of wet curing (i.e., at 100% humidity). Additional mechanical and physical properties that are relevant for construction applications (i.e., setting time, void content, modulus of elasticity, and Poisson's ratio) are investigated for a select composition that appears to be particularly promising (based on strength, volumetric expansion, and cost considerations) for outdoor and underwater construction applications. For this composition, curing time-compressive strength and curing time-volumetric expansion relationships are also proposed. The study presented in this paper is part of a wider research effort to demonstrate the feasibility and improve the performance of FG-based blends for outdoor and underwater construction applications [19,20,24]. Investigation of the water solubility of these blends is a major component of this effort [24], but it is out of the scope of the present paper.

3. Dependence of strength and volumetric expansion on composition

In this study, compressive strength and volumetric expansion were considered as the critical parameters to identify appropriate composition ranges of FG-based blends for outdoor/underwater applications. In fact, compressive strength is a crucial mechanical property that controls the load-carrying capacity of a structural material. The volumetric expansion, which generally occurs due to delayed formation of ettringite [25,16], is an important property related to the durability of the material and is commonly associated with significant strength deterioration and even integrity loss due to formations of cracks inside the blend, and with potential damage to adjacent materials. However, the expansion of a blend could also be a useful property for some specific applications, e.g., expansive concrete can be used to compensate for drying shrinkage [26]. In this study, the focus is on short-term properties of the material and, thus, only expansion during curing is considered, whereas expansion under prolonged water immersion, albeit important, was considered out of the scope of the paper. It is noteworthy that internal and/or invisible cracks can also have an important effect on the mechanical properties and the durability of the material under consideration. However, since they are more complex to investigate than visible cracks, they were also deemed out of the scope of this investigation on strength and durability of FG-based blends, considering its preliminary nature. This section of the paper describes the methodology followed to investigate these properties and illustrates the results of the investigation.

3.1. Methodology

The following tasks were performed to investigate the dependence of compressive strength and volumetric expansion on the relative content of pH-adjusted FG, FA, and PC: (1) component raw materials were characterized both at the microscopic and macroscopic levels; (2) compressive strength and volumetric expansion were experimentally measured for a wide range of compositions with high pH-adjusted FG content using a classic mixture method to define the experimental matrix; (3) RSMs were developed for both compressive strength and volumetric expansion; and (4) appropriate composition ranges were identified and a specific composition was selected for further investigation. Characterization of the raw materials is a necessary step to provide a baseline understanding of the material composition and morphology. This characterization is particularly important for the pH-adjusted FG because it is a by-product material obtained without a rigorous quality control of its production. It also enables researchers to compare the results presented in this paper with those of other studies available in the literature by accounting for potential differences in the base materials.

The experimental measurement of compressive strength and volumetric expansion provides the data points for the development of RSMs based on a test matrix properly selected to explore compositions with high pH-adjusted FG content. These RSMs can be used to: (1) predict the compressive strength and volumetric expansion of compositions without additional expensive and time-consuming physical testing, (2) investigate appropriate composition ranges for the proposed FG-based blends with promising properties for the construction applications of interest, and (3) select specific compositions for different applications, e.g., by using the RSMs as objective or constraint functions for numerical optimization approaches.

3.2. Raw materials characterization

The pH-adjusted FG used in this research was obtained from the stockpiles located in Geismar, LA (USA). This material was obtained by using circulating fluidized bed combustion (CFBC) ash as the alkali material for neutralization of the FG. A sample of pH-adjusted FG was analyzed using X-ray diffraction (XRD) to investigate the crystallographic composition, scanning electron microscopy (SEM) to analyze the microscopic morphology, and grain size analysis to identify the granulometry of the material. The characterization of this raw material is a crucial component to ensure repeatability of the results presented in this work, since the pH-adjusted FG material used here is an industrial by-product and, thus, can present a very high variability in its composition and crystallography. In the XRD pattern shown in Fig. 1(a), the higher peaks (with higher intensity) correspond to gypsum (G: $CaSO_4{\cdot}2H_2O$), whereas the lower peaks represent anhydrite (A: $CaSO_4$), fluorite (F: CaF_2), and quartz (Q: SiO_2). Grain size distribution of the pH-adjusted FG was identified by following the procedure described in ASTM D6913 [31]. The grain distribution curve shown in Fig. 1(b) is based on sieve analysis results only (i.e., for grains larger than or equal to 0.075 mm), because the employed FG material is soluble in water and, thus, the hydrometric test for identification of smaller grains is inapplicable. It is observed that about 7% of the pH-adjusted FG is composed by grains with size comparable to that of coarse aggregate. The SEM image provided in Fig. 2(a) shows that the majority of the crystals in the pH-adjusted FG sample are prismatic gypsum crystals. The pH of the material was identified as per ASTM D4972 standard test procedure [32]. The sample mean of pH for 20 pH-adjusted FG samples was found equal to 7.90 with a sample standard deviation of 0.08.

Class C fly ash (FA) was supplied by the Big Cajun II Power Plant located in New Roads, LA (USA). Fig. 2(b) displays an SEM image of an FA sample, which shows the spherical shape of the FA particles. Type II Portland cement (PC) was obtained from a local supplier. The results of the XRD analysis based on the Rietveld method [27] for one representative sample of pH-adjusted FG, FA, and PC are reported in Table 1. It is noteworthy that testing different batches of the pH-adjusted FG can provide different strength and durability properties depending on the natural variability of the fluorspar used to produce FG, the amount of alkali material used for neutralization, and the duration of weather exposure of the stockpiled material. For the pH-adjusted FG provided by the supplier, determination of the exact amount of CFBC ash used for pH adjustment was not possible. Thus, only one batch of this material was used in this study to minimize the variability induced by the potential differences in CFBC ash content.

3.3. Investigation of compressive strength and volumetric expansion

3.3.1. Specimen preparation

The pH-adjusted FG was dried at a temperature of 45 °C for a period of 14 h before preparation of the experimental specimens, following the recommendations of standard ASTM D2216 [28] to remove the free water without inducing dehydration of the gypsum. The dry components of pH-adjusted FG, FA, and PC were machine mixed together into a homogeneous blend. This blend was mixed with water to obtain a uniform mixture and then molded into cylinders of 10.15 cm × 20.3 cm (4 in × 8 in) size by following ASTM C192 standard [29]. The cylindrical specimens

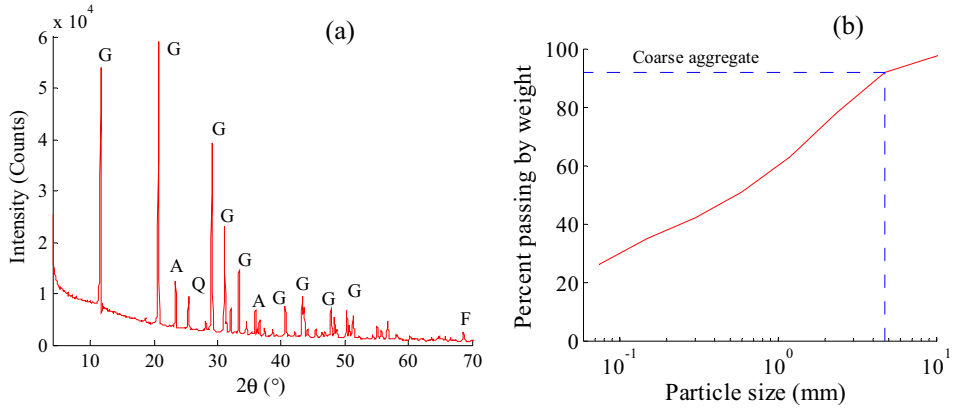

Fig. 1. Characterization of pH-adjusted FG: (a) X-ray diffractogram of a pH-adjusted FG sample (G: gypsum, A: anhydrate, F: fluorite, Q: quartz), and (b) grain size distribution of pH-adjusted FG material.

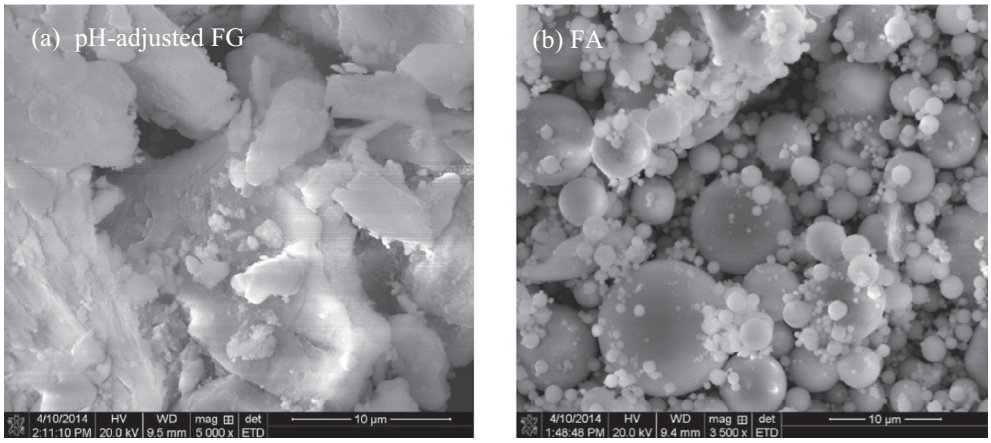

Fig. 2. SEM images: (a) pH-adjusted FG, and (b) FA.

Table 1
Crystallographic compositions of FG, FA, and PC (% by dry weight).

Components	FG	FA	PC
Akermanite: $Ca_2Mg(Si_2O_7)$	–	32.6	–
Alite: $3CaO.SiO_2$	–	–	70.4
Anhydrite: $CaSO_4$	5.7	6.8	–
Brownmillerite: $Ca2(Al,Fe)_2O_5$	–	29.4	23.3
Fluorite: CaF_2	0.8	–	–
Gypsum: $CaSO_4{\cdot}2H_2O$	93.4	–	1.4
Periclase: MgO	–	5.9	–
Perovskite: $CaTiO_3$	–	3.9	–
Quartz: SiO_2	0.1	20.3	–
Calcite: $CaCO_3$	–	–	4.9

were de-molded after 24 h and cured at 100% humidity and 23 ± 2.0 °C for a curing period of 28 days. The amount of water used in mixing the blend was kept constant and equal to 20% of the total weight of dry material in order to investigate the effects of the blend composition on the properties of the hardened material independently from the water/cement content. The constant amount of water used in this research was determined based on the workability of the material and corresponded to the minimum amount of water that ensured sufficient workability for all compositions considered (Table 2).

Table 2
Mixture proportions of dry components (i.e., pH-adjusted FG, FA, and PC) for FG-based blend.

Designation	Mix composition (% by dry wt.)		
	w_{FG}	w_{FA}	w_{PC}
D_1	60	38	2
D_2	60	34	6
D_3	60	30	10
D_4	70	28	2
D_5	70	24	6
D_6	70	20	10
D_7	80	18	2
D_8	80	14	6
D_9	80	10	10
D_{10}	90	8	2
D_{11}	90	4	6
D_{12}	90	0	10
C_1	73	25	2
C_2	62	35	3
C_3	75	18	2

3.3.2. Experimental matrix selection

The FG-based blends proposed in this study consist of three individual dry cementitious material components (i.e., pH-adjusted FG, FA, and PC). The compressive strength and volumetric expansion were investigated by assuming that their values depend only on the composition of the mixture, i.e., by considering a mixture problem [30]. It is noted that the pH-adjusted FG used in this research is a mix of FG and CFBC ash, in which the content of CFBC ash varies between 2% and 5% from batch to batch (G. Mitchell, Brown Industries, personal communication 2016). The separate effects of the variability in CFBC ash content and of the FG composition were not explicitly investigated here, but it is likely that they would increase the dispersion of the experimental results when compared to those reported in this research.

The focus of this paper is investigating high-strength mixtures with high content of pH-adjusted FG. Thus, the following composition ranges were experimentally investigated:

$$\begin{aligned} 60\% &\leqslant w_{FG} \leqslant 90\% \\ 0\% &\leqslant w_{FA} \leqslant 38\% \\ 2\% &\leqslant w_{PC} \leqslant 10\% \end{aligned} \tag{2}$$

in which w_{FG}, w_{FA}, and w_{PC} denote the percentages of dry weight of pH-adjusted FG, FA, and PC, respectively, with respect to the total weight of dry material.

The experimental matrix with the proportions of the dry components used to fabricate the FG-based blend is reported in Table 2. Twelve compositions (designated as D_1 through D_{12} in Table 2) were used as fitting data points to develop predictive RSMs. For each of the 12 compositions, a set of five cylindrical specimens was prepared to study the effect of composition on compressive strength and volumetric expansion. Three additional compositions (designated as C_1 through C_3 in Table 2) were used as control data points to validate the developed predictive models. These three control points correspond to blends with low amounts of cement and were chosen to validate the models in the region of lower cost of the blends, which is the region of most practical interest. Five cylindrical specimens were also prepared for each of these three compositions. Hereinafter, each composition is identified by the designation reported in Table 2 followed by three numbers in parentheses separated by dashes and indicating the values of w_{FG}, w_{FA}, and w_{PC}, respectively, corresponding to the considered composition.

3.3.3. Testing procedures

The testing procedures used for this research were selected based on the goal of developing a FG-based blend as a substitute

for ordinary concrete and/or limestone in outdoor and underwater applications. Thus, the test methods commonly used for ordinary concrete were also employed to investigate compressive strength and volumetric expansion of the different FG-based blend compositions. It is noted here that the proposed material is a concrete system, which after hardening contains binding material, water, air, fine aggregate, and coarse aggregate (see Fig. 3). Compressive strength tests were conducted following the method described in the ASTM C39 standard for concrete specimens [33]. The relative volumetric expansion after 28 days of curing (η) was calculated as the ratio between the change in volume and the initial volume, i.e.,

$$\eta = (V_2 - V_1)/V_1 \quad (3)$$

where V_1 and V_2 denote the volume of each specimen immediately after demolding and after 28 days of curing, respectively. The specimens' volumes were obtained using a graduated cylinder following the ASTM C1005 standard [34]. It is noted here that ASTM does not provide a standard for volumetric expansion of the material considered in this study. In particular, the ASTM standards for expansion measurement of cement mortars (i.e., ASTM C806 [35]) and shrinkage-compensating concretes (ASTM C878 [36]) cannot be directly used for the FG-based blends. Since any modifications of these standards would require significant investigations to verify their consistency (e.g., [37–39]), the simpler approach described above and based on elementary principles was preferred for this preliminary study.

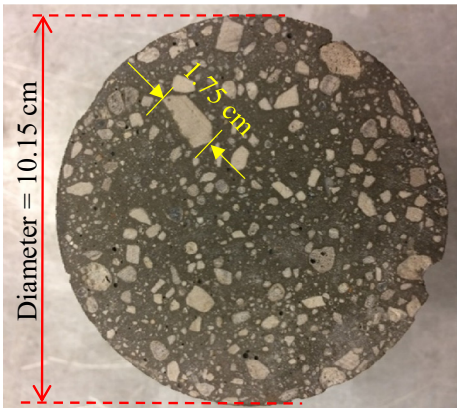

Fig. 3. Representative cross-section of a hardened cylindrical sample of FG-based blend.

3.3.4. Experimental results

The sample mean (μ), sample standard deviation (σ), and coefficient of variation (COV) values of compressive strength (f_c) and relative volumetric expansion (η) for the different compositions (separated between fitting and control data points) are reported in Table 3. The presence of cracks visible to the unaided eye on the specimens before testing is also reported as an indirect indicator of excessive expansion. It was observed that the compressive strength decreases considerably with increasing w_{FG} when w_{PC} is equal to 2% and 6%, i.e., with a reduction in μ_{f_c} equal to 8.4 MPa and 11.9 MPa, respectively, when w_{FG} increases from 60% to 90%. The decrease in μ_{f_c} is less pronounced and non-monotonous for w_{PC} equal to 10%, with a reduction in μ_{f_c} equal to 3.3 MPa when w_{FG} increases from 60% to 90%. The maximum and minimum values of μ_{f_c} for different amounts of w_{PC} are always attained at w_{FG} equal to 60% and 90%, respectively. A similar trend in μ_{f_c} cannot be identified for constant values of w_{PC} and the maximum and minimum values of μ_{f_c} are attained for various w_{PC} depending on w_{FG}. The coefficient of variation of the compressive strength (COV_{f_c}) changes considerably among different compositions. The maximum COV_{f_c} value is 30.9% and is observed for composition D_4 (70-28-2), whereas the minimum COV_{f_c} value is 4.1% and is observed for D_9 (80-10-10). Also for this quantity, a trend cannot be easily identified. However, it is observed that the values of COV_{f_c} tend to be relatively smaller and change less for compositions with w_{PC} equal to 10% than for compositions with other contents of cement.

Regarding the relative volumetric expansion (η), μ_η tends to increase when w_{PC} increases and w_{FG} is equal to 60%. For other values of w_{FG}, the maximum values of μ_η occur always at w_{PC} equal to 6%. The range of variability for COV_η was similar to that measured for COV_{f_c}, i.e., $4.1\% \leq COV_{f_c} \leq 35.5\%$. The maximum COV_η value is 35.5% and is observed for composition D_1 (60-38-2), whereas the minimum COV_{f_c} value is 4.1% and is observed for D_3 (60-30-10).

It was also found that f_c and η are negatively correlated with a correlation coefficient $\rho_{f_c,\eta}$ equal to −0.55, with compositions D_2 (60-34-6) and D_1 (60-38-2) corresponding to the two highest values for μ_{f_c} (i.e., 13.8 MPa and 10.8 MPa, respectively) and the two lowest values for μ_η (i.e., 2.7% and 2.2%, respectively). This negative correlation can be observed from the trend line presented in Fig. 4, where the average compressive strength is plotted versus the average relative volumetric expansion for all tested compositions. The visual inspection of the specimens indicates that the specimens for all compositions with $\mu_\eta \leqslant 6.3\%$ did not present

Table 3
Experimental results for f_c and η of FG-based compositions.

Data point classification	Composition (w_{FG}-w_{FA}-w_{PC})	μ_{f_c} (MPa)	σ_{f_c} (MPa)	COV_{f_c} (%)	μ_η (%)	σ_η (%)	COV_η (%)	Visible Cracks
Fitting data points	D_1 (60-38-2)	10.8	1.1	10.2	2.2	0.8	35.5	No
	D_2 (60-34-6)	13.8	1.5	11.0	2.7	0.9	29.3	No
	D_3 (60-30-10)	5.5	0.4	6.9	12.3	0.5	4.1	Yes
	D_4 (70-28-2)	5.3	1.6	30.9	6.1	1.3	20.6	No
	D_5 (70-24-6)	3.5	0.7	19.2	16.3	1.1	6.4	Yes
	D_6 (70-20-10)	3.4	0.2	7.1	8.5	1.6	18.5	Yes
	D_7 (80-18-2)	3.6	0.4	10.1	8.3	2.0	24.5	No
	D_8 (80-14-6)	2.5	0.2	8.2	11.7	0.6	5.4	Yes
	D_9 (80-10-10)	4.5	0.2	4.1	5.2	0.8	15.8	No
	D_{10} (90-8-2)	2.4	0.1	5.9	3.3	0.5	13.6	No
	D_{11} (90-4-6)	1.8	0.3	20.1	9.6	1.4	14.9	Yes
	D_{12} (90-0-10)	2.2	0.2	7.4	6.3	1.2	18.9	No
Control data points	C_1 (73-25-2)	4.4	0.9	21.5	8.1	0.5	6.3	Yes
	C_2 (62-35-3)	8.9	0.6	6.8	4.1	0.6	15.2	No
	C_3 (75-18-2)	4.0	0.5	13.3	8.3	1.4	17.1	Yes

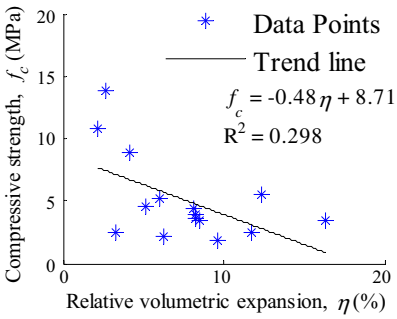

Fig. 4. Correlation between experimental values of μ_{f_c} and μ_η.

any visible cracks before compression testing (e.g., see Fig. 5(a) for composition C_2 (62-35-3) with μ_η equal to 4.1%). Conversely, the specimens for all other compositions (i.e., with $\mu_\eta \geqslant 8.1\%$) had visible cracks (e.g., see Fig. 5(b) for composition D_5 (70-24-6) with μ_η equal to 16.3%), with the exception of the specimens corresponding to composition D_7 (80-18-2), for which μ_η is equal to 8.3% and no cracks were visible before testing (see Fig. 5(c)).

3.3.5. Discussion of results

As previously observed, the values of μ_{f_c} and μ_η depend on w_{PC} and w_{FG} in a nonlinear and non-monotonic manner. This phenomenon can be partially explained by the combination of competing effects that take place when w_{PC} is increased and are related to the formation of ettringite: (1) the production of ettringite due to reaction between gypsum and cement during the early hydration phases fills in pores and voids of the porous gypsum structure to form a denser matrix, and (2) delayed production of ettringite leads to a high volumetric expansion and eventually deterioration of the strength [40]. It is hypothesized that the same two competing mechanisms affecting μ_{f_c} and μ_η are also influencing their variability, COV_{f_c} and COV_η, i.e., the production of early ettringite tends to reduce the values of COV_{f_c} and COV_η, whereas the production of late ettringite tends to increase the values of COV_{f_c} and COV_η. However, the further investigations that would be needed to test this hypothesis are outside the scope of this paper. The presence of visible cracks for the higher values of μ_η also partially explains the negative correlation between compressive strength and relative volumetric expansion observed in Fig. 4, since the presence of visible cracks leads to a reduction in compressive strength.

3.3.6. Response surface model development

Two RSMs were developed by fitting the coefficients of a polynomial function of the percentage of PC and pH-adjusted FG to the sample means of the experimentally measured compressive strengths and relative volumetric expansions (see Table 3). Least squares fitting was employed via the "sftool" MATLAB toolbox [41]. The independent variables were scaled as $x = w_{PC}/10$ and $y = w_{FG}/100$ in order to minimize the round-off error [42]. The following polynomial expressions are proposed for the RSM of the compressive strength and relative volumetric expansion:

$$\hat{f}_c(x,y) = \sum_{i=0}^{2}\sum_{j=0}^{3}(a_{ij}x^i y^j);\ 0.2 \leqslant x \leqslant 1;\ 0.6 \leqslant y \leqslant 0.9 \quad (4)$$

$$\hat{\eta}(x,y) = \sum_{i=0}^{2}\sum_{j=0}^{3}(b_{ij}x^i y^j);\ 0.2 \leqslant x \leqslant 1;\ 0.6 \leqslant y \leqslant 0.9 \quad (5)$$

respectively, in which $\hat{f}_c$ and $\hat{\eta}$ denote the numerical estimate of the FG-based blend's compressive strength (in MPa) and relative volumetric expansion (in%), respectively; and a_{ij} and b_{ij} (the numerical values of which are reported in Table 4) denote the polynomial coefficients for the two RSMs obtained from the surface fitting procedure. It is noted here that the selected polynomial expressions are exact fits to the fitting data points. Reducing the order of the polynomials was found to produce relatively large differences between the experimental results and the RSM estimates at the fitting data points (e.g., up to 53.8% errors for $\hat{f}_c$ and up to 38.5% errors for $\hat{\eta}$ when using a quadratic model with nine coefficients). It was also verified that the fitted RSMs do not exhibit extreme oscillatory behaviors within the fitting data points, which would be an indication of overfitting [43]. It is also noted that different fitting techniques (i.e., parametric fitting) and RSM functional expressions

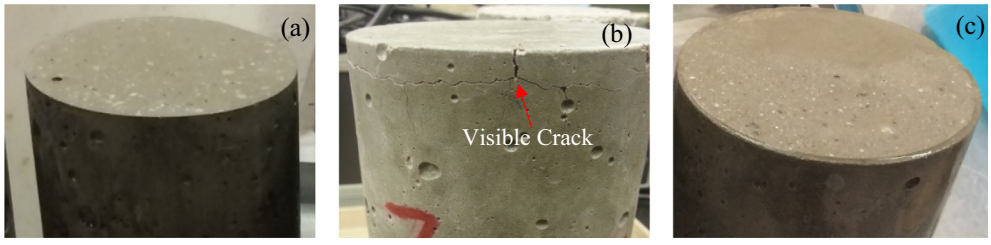

Fig. 5. Visual inspection of different specimens before compressive strength test: (a) composition C_2 (62-35-3) sample with no visible cracks and $\mu_\eta = 4.1\%$, (b) composition D_5 (70-24-6) sample with visible cracks and $\mu_\eta = 16.3\%$, and (c) composition D_7 (80-18-2) sample with no visible cracks and $\mu_\eta = 8.3\%$.

Table 4
Coefficients of the RSMs for $\hat{f}_c$ and $\hat{\eta}$.

	$i=0, j=0$	$i=0, j=1$	$i=0, j=2$	$i=0, j=3$	$i=1, j=0$	$i=1, j=1$
a_{ij}	-219.59	860.93	−1069.19	430.56	3134.54	−11625.61
b_{ij}	2434.38	−9856.51	13156.89	−5794.33	−12992.15	51481.48
	$i=1, j=2$	$i=1, j=3$	$i=2, j=0$	$i=2, j=01$	$i=2, j=02$	$i=2, j=3$
a_{ij}	14220.06	−5751.71	−2459.64	8928.03	−10678.63	4221.16
b_{ij}	−67094.12	28868.08	10384.34	−40743.85	52593.63	−22422.13

(e.g., Gaussian and exponential models), as well as fitting the RSM to all sample measurements instead of to the mean values, were investigated. However, the RSMs presented here were the ones with the best predictive capabilities for the parameters of interest.

Fig. 6 (a) and (b) plot the RSMs of $\hat{f}_c$ and $\hat{\eta}$ and compare them with the experimentally derived sample mean compressive strength and relative volumetric expansion, respectively, at the three control points C_1 (73-25-2), C_2 (62-35-3), and C_3 (75-18-2) (identified by red triangular markers). The sample mean values of compressive strength and relative volumetric expansion at the fitting data points are also reported and are identified by black dots. The robustness of the RSMs with respect to random errors in the component amounts due to weight measurement tolerance (i.e., ±0.3333% for pH-adjusted FG and ±0.0006% for PC) was evaluated by using Monte Carlo simulation. In particular, 10,000 error samples were randomly generated by assuming a uniform distribution of the measurement errors at each fitting point. For each of these samples, a new RSM model was fitted and the compressive strengths at the control points (with randomly simulated errors in the compositions) were recalculated. Table 5 reports the RSM-based estimates of the compressive strength, $\hat{f}_c$, and relative volumetric expansion, $\hat{\eta}$, with their corresponding 95% confidence intervals, as well as the relative errors in compressive strength, $\delta_{\hat{f}_c}$, and relative volumetric expansion, $\delta_{\hat{\eta}}$, with their corresponding 95% error margins. The variability of the predicted $\hat{f}_c$ and $\hat{\eta}$ values due to the effects of weight measurement tolerance on the RSMs is significantly lower than the natural variability (i.e., sample standard deviation) measured in the experimental tests for both compressive strength and volumetric expansion (see Table 3). This result suggests that the developed RSMs for $\hat{f}_c$ and $\hat{\eta}$ can be used for predicting the expected values of compressive strength and volumetric expansion within the ranges $2\% \leqslant w_{PC} \leqslant 10\%$ and $60\% \leqslant w_{FG} \leqslant 90\%$. It is also noted here that the variability of the RSM-based estimates at the fitting data points due to random errors in the components' weight measurement is negligible for both $\hat{f}_c$ and $\hat{\eta}$.

3.4. Identification of appropriate composition ranges for outdoor and underwater applications

The FG-based blends considered in this study were investigated for construction of breakwaters for coastal protection applications. This type of structures is expected to resist wave and current loads in addition to self-weight and hydrostatic pressure. According to the design methodology described in the Coastal Engineering Manual (CEM) [44] and Van Der Meer and Sigurdarson [45], the breakwater's height should be selected to avoid overtopping of the breakwater by the sea waves. By assuming a water depth of 4 m, soft soil depth of 5 m, and significant wave height of 0.65 m in the coastal regions of Louisiana, a breakwater designed for these conditions could reach a height of 14 m [46,47]. By further assuming that the core of the breakwater is made of FG-based blend and that the load carrying contact area for the core material is 30% of its total horizontal cross-sectional area, using a safety factor equal to four, the compressive strength for the FG-based blend for this application should be higher than or equal to about 4.0 MPa (580 psi). However, it should be noted that this value is a conservative estimate of the compressive strength requirements for the FG-based blend in breakwater construction and that the identification of the appropriate compressive strength for this type of application is outside the scope of the paper. Based on the experimental results reported in the previous sections of this paper, the maximum relative volumetric expansion, η, of the FG-based blend should be lower than 6% (see Table 3) in order to avoid possible cracking, which would produce initiation points for the fracture of the material and, thus, make the breakwater structure more vulnerable to leaching and wave loads. Based on the above considerations, appropriate ranges for w_{PC}, w_{FG}, and w_{FA}, were identified using the developed RSMs for $\hat{f}_c$ and $\hat{\eta}$. Fig. 7 shows the contour lines of the RSMs corresponding to $f_c = 4$ MPa and $\eta = 6\%$ and the two regions (identified by the portions of the plot that are not hatched) that contain the ranges of w_{PC} and w_{FG} that are appropriate for the proposed application. One region corresponds to low values of w_{PC} and w_{FG}, whereas the second region corresponds to high values of

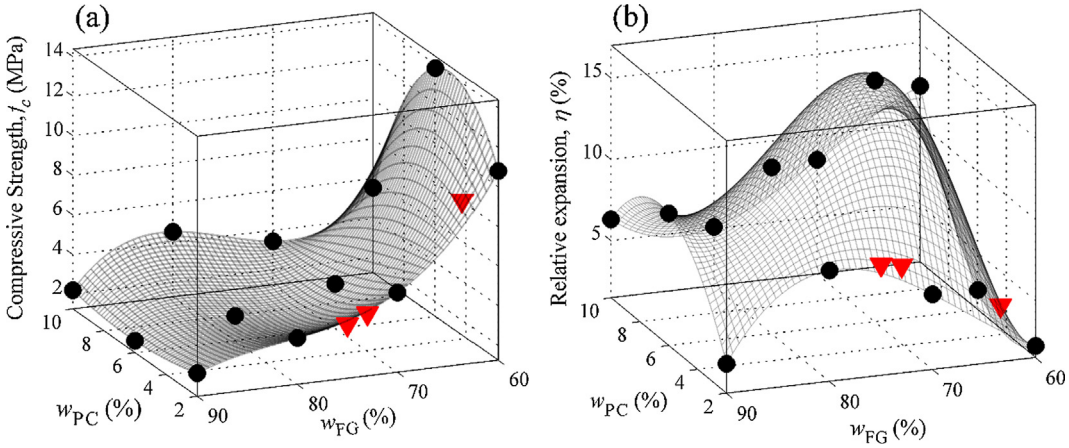

Fig. 6. RSMs: (a) f_c, and (b) η. ●: fitting data points, ▼: control data points.

Table 5
Comparison of control experimental data points and RSM results: estimates of compressive strenght, $\hat{f}_c$, and relative volumetric expansion, $\hat{\eta}$, with corresponding 95% error margins, and relative errors, $\delta_{\hat{f}_c}$ and $\delta_{\hat{\eta}}$, with corresponding 95% error margins.

Composition (w_{FG}-w_{FA}-w_{PC})	$\hat{f}_c$ (MPa)	$\delta_{\hat{f}_c}$ (%)	$\hat{\eta}$ (%)	$\delta_{\hat{\eta}}$ (%)
C_1 (73-25-2)	4.5 ± 0.1	3.20 ± 2.75	7.2 ± 0.2	−11.24 ± 2.09
C_2 (62-35-3)	10.2 ± 0.5	15.36 ± 5.28	4.2 ± 0.6	2.58 ± 14.06
C_3 (75-18-2)	4.2 ± 0.1	4.53 ± 2.30	7.8 ± 0.1	−6.54 ± 1.54

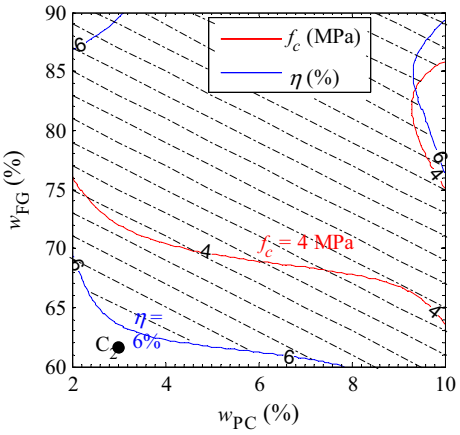

Fig. 7. Contour plot of RSMs for $\hat{f}_c$ = 4 MPa and $\hat{\eta}$ = 6%. ●: composition C_2 (62-35-3).

w_{PC} and values of w_{FG} that are close to 80%. Among the compositions in the region corresponding to low values of w_{PC} and w_{FG}, composition C_2 (62-35-3) (identified by a black dot in Fig. 7) was selected for further investigation since it met the required conditions (i.e., μ_{f_c} = 8.9 MPa greater than 4 MPa and μ_η = 4.1% less than 6%).

4. Further studies on composition C_2 (62-35-3)

In the second phase of this study, the following mechanical and physical properties were investigated for the selected composition C_2 (62-35-3), in order to investigate its application potential: (1) modulus of elasticity and Poisson's ratio, which are mechanical properties needed to characterize the material for structural analysis (e.g., via finite element analysis); (2) initial and final setting times, which correspond to the time after which a hardening material loses its plasticity (i.e., it cannot be formed any more) and gains enough strength to begin final finishing, respectively; (3) dry density, i.e., weight per unit volume of the dry material; (4) void content, which can be used as a measure of non-uniformity in a concrete and can affect several mechanical properties such as fatigue resistance, water penetration, and weathering; and (5) bulk density of the material after it is crushed. In addition, the effect of curing time on compressive strength and relative volumetric expansion were also experimentally investigated. Following the presentation of the experimental results, a brief discussion of the appropriateness of composition C_2 (62-35-3) for outdoor and underwater applications when compared to ordinary concrete is also provided.

4.1. Chord modulus of elasticity and Poisson's ratio

The chord modulus of elasticity (E) and Poisson's ratio (ν) were measured for the FG-based composition C_2 (62-35-3) based on the procedure described in the ASTM C469 standard [48]. Five cylindrical specimens were subjected to four loading cycles between 1% and 40% of the sample mean compressive strength estimated from compressive strength tests. All specimens of FG-based blend remained approximately linear elastic within these load levels. The values of E ranged between 7.53 GPa and 9.49 GPa, with a sample mean μ_E equal to 8.66 GPa and a sample standard deviation σ_E equal to 0.83 GPa; whereas the values of ν ranged between 0.17 and 0.19, with a sample mean μ_ν equal to 0.18 and a sample standard deviation σ_ν equal to 0.01.

4.2. Setting time

The initial and final setting times of composition C_2 (62-35-3) were identified using three sample specimens according to the procedure described in the ASTM C403 standard [49]. The average initial and final setting times were equal to 131 min and μ_{t_f} equal to 325 min, respectively, with sample standard deviations equal to σ_{t_i} equal to 8 min and σ_{t_f} equal to 7 min, respectively.

4.3. Dry density, void content, and bulk density

The dry density (ρ_d) and void contents (n) were determined by following the procedure specified by the ASTM C1754 standard [50]. Five specimens of composition C_2 (62-35-3) were tested and the average dry density and void content were estimated as μ_{ρ_d} equal to 1750 kg/m^3 and μ_n equal to 9.3%, respectively, with sample standard deviations of σ_{ρ_d} equal to 7 kg/m^3 and σ_n equal to 0.3%, respectively.

The bulk density (ρ) of the FG-based blend after crushing was determined by following the procedure specified by the ASTM C29 standards [51]. Five specimens of composition C_2 (62-35-3) were crushed to grain sizes of 1 to 5 cm and the bulk density was calculated. The sample mean and sample standard deviation of the bulk density were estimated as μ_ρ equal to 963 kg/m^3 and σ_ρ equal to 41 kg/m^3, respectively.

4.4. Curing time effects on volumetric expansion and compressive strength

A total of 20 identically prepared specimens of composition C_2 (62-35-3) were used to investigate the effect of curing time on compressive strength, f_c, and relative volumetric expansion, η. Four sets of five cylindrical specimens were tested for compressive strength and relative volumetric expansion after 7, 14, 28, and 56 days of curing, respectively. The experimental results from these tests are reported in Table 6. As expected, it is observed that the specimens gain strength at a high rate at the beginning of the curing process, and that this rate decreases with time. In fact, the FG-based blend reached a 5.0 MPa compressive strength after the first 7 days of curing, which corresponds to 56% of the measured compressive strength after 28 days, and gained 1.3 MPa of additional compressive strength in the second 7 days of curing. It is also observed that the compressive strength gain is still significant after 28 days of curing, with an additional increase in compressive strength equal to 1.6 MPa between 28 and 56 days of curing (i.e., almost 18% of the 28-day compressive strength). This gain of strength with the curing period indicates that the porous gypsum matrix that develops in the early curing phase is gradually filled in by hydration products such as ettringite. It is observed that the increased rate for the relative volumetric expansion follows a similar trend as the increased rate for the compressive strength, i.e., it is higher at the beginning of the curing time and gradually reduces to almost zero after 28 days of curing. In fact, a relative volumetric expansion of 2.3% was measured after 7 days of curing, an increment of 1.7% was measured between 7 and 14 days of cur-

Table 6
Curing effects on compressive strength and relative volumetric expansion of composition C_2 (62-35-3).

Day	μ_{f_c} (MPa)	σ_{f_c} (MPa)	μ_η (%)	σ_η (%)
7	5.0	0.3	2.3	0.3
14	6.3	0.6	4.0	0.3
28	8.9	0.6	4.1	0.6
56	10.6	1.2	4.2	0.5

ing, and an increment of only 0.1% was measured between 28 and 56 days of curing. The formation of ettringite due to the reactions between pH-adjusted FG and PC could be responsible for the relative volumetric expansion and its rate of increase. However, additional tests (including chemical analysis and XRD) are needed to verify this hypothesis.

4.5. Discussion of experimental results for composition C_2 (62-35-3)

The experimentally measured properties of the selected composition C_2 (62-35-3) are discussed in terms of the potential use of this FG-based blend as a substitute for ordinary concrete in outdoor and underwater construction, as well as for granular materials commonly employed for construction of artificial reefs, such as recycled crushed concrete and crushed limestone. Thus, first the mechanical and physical properties of this FG-based blend are compared with those of ordinary concrete when considered as continua, and then with those of granular materials. It is noteworthy that composition C_2 (62-35-3) has a very low dissolution rate in water, with an effective diffusion coefficient of 4.54×10^{-13} m^2 s^{-1} at room temperature (21 ± 2 °C), in contrast with natural gypsum and FG, which have significantly higher effective diffusion coefficients in water equal to 1.0×10^{-9} m^2 s^{-1} [52] and 4×10^{-10} m^2 s^{-1} [53], respectively, and are not appropriate for outdoor and underwater construction.

The mechanical properties of the FG-based blend corresponding to composition C_2 (62-35-3) compare to those of Portland cement concrete as follows: (1) the sample mean compressive strength of the FG-based blend is $\mu_{f_c} = 8.9$ MPa, which is significantly lower than the common range of compressive strength for Portland cement concrete, i.e., 20–40 MPa [54]; (2) the sample mean modulus of elasticity of the FG-based blend is $\mu_E = 8.7$ GPa, which is also lower than the common range for ordinary concrete, i.e., 21–40 GPa; and (3) the sample mean Poisson's ratio of the FG-based blend is $\mu_\nu = 0.18$, which is within the common range for ordinary concrete, i.e., 0.15–0.20 [54].

The physical properties of the FG-based blend corresponding to composition C_2 (62-35-3) compare to those of Portland cement concrete as follows: (1) the sample mean relative volumetric expansion of the FG-based composite binder during curing is 4.1%, which is significantly larger than that of ordinary concrete (i.e., usually less than 1%) [54]; (2) the sample mean dry density of the FG-based blend is 1750 kg/m^3, which is significantly lower than that of ordinary concrete, i.e., 2200–2400 kg/m^3 [54]; and (3) the average initial and final setting times of the FG-based blend are μ_{t_i} = 130 min and μ_{t_f} = 325 min, which are lower than the ranges for the corresponding quantities for ordinary concrete, i.e., 180–510 min for the initial setting time, and 360–670 min for the final setting time [54]. The compressive strength gain of the FG-based blend is still significant after 28 days of curing, with an additional increase in compressive strength equal to 1.6 MPa between 28 and 56 days of curing, i.e., an increase of almost 18% of the 28-day compressive strength, compared with the 3% to 15% increase commonly observed in ordinary concrete during the same period [54].

From the presented comparison, it is suggested that the considered FG-based blend can be used in outdoor and underwater applications with low strength and low stiffness requirements (e.g., artificial reefs armored with limestone cover), in which initial expansion can be considered a positive effect or at least is not a concern, and quick setting is desirable. Such applications include small non-structural soil retaining walls, sidewalks, and decorative elements.

The use of the considered FG-based blend in granular form for construction of artificial reefs is also of significant interest. In fact, this structural typology can be built using low-strength aggregates that are insoluble in water. Crushed recycled concrete and limestone are commonly used as construction materials for this application. However, in the US Gulf Coast region and particularly in Louisiana, these materials presents two severe drawbacks: (1) they are expensive due to their limited local availability and need for lengthy transportation [23]; and (2) they are heavy, with bulk densities of 1265–1380 kg/m^3 for crushed recycled concrete [55] and of 1200–1450 kg/m^3 for crushed limestone with grain sizes of 1–5 cm [55] and, thus, tend to quickly sink in the soft sea bed near the coast [56]. The crushed FG-based blend corresponding to composition C_2 (62-35-3) has an average bulk density of 963 kg/m^3 for grain sizes of 1–5 cm, which represents a reduction of 20%–33% of the material unit weight. From an economical point of view, the total cost (i.e., the sum of material and transportation costs) of the FG-based blend corresponding to composition C_2 (62-35-3) is expected to be significantly lower than the total cost of crushed limestone. Therefore, it appears that the considered FG-based blend could be beneficially used for construction of artificial reefs, e.g., in Louisiana.

5. Conclusions

In this paper, compressive strength and relative volumetric expansion of a fluorogypsum-based blend were experimentally investigated by considering different proportions of the dry components, i.e., pH-adjusted fluorogypsum (FG), fly ash (FA), and Portland cement (PC). The pH-adjusted FG content was varied between 60% and 90% of the dry material weight, whereas the PC content was varied between 2% and 10% of the dry material weight. From the experimental results, it was observed that (1) the compressive strength decreases considerably for increasing content of pH-adjusted FG when the PC content is equal to 2% and 6%, whereas this decrease is less pronounced and non-monotonous for PC content equal to 10%; (2) the maximum and minimum values of compressive strength for different amounts of PC are always attained for pH-adjusted FG contents of 60% and 90%, respectively; (3) volumetric expansions greater than 6.3% correspond to the formation of visible cracks on the specimens; (4) compressive strength and relative volumetric expansion are negatively correlated with a correlation coefficient equal to -0.55.

Two response surface models (RSMs) were developed and used for the prediction of the compressive strength and relative volumetric expansion of different compositions. The precision and the accuracy of these models were validated by using three control data points. Using these RSMs, appropriate composition ranges were identified by considering the construction of breakwaters as an application. Among the acceptable compositions in terms of minimum strength and maximum relative volumetric expansion, a composition containing 62% pH-adjusted FG, 35% FA, and 3% PC was further investigated in terms of modulus of elasticity, Poisson's ratio, initial and final setting times, dry density, void contents, and effect of curing time on the compressive strength. These additional experimental results indicated that the considered composition appears to be a promising low-cost material for specific outdoor and underwater construction applications with low strength and low stiffness requirements, as well as for construction of artificial reefs along the US Gulf Coast region. However, it is highlighted here that further research is needed to investigate other properties of this material, such as underwater expansion and long-term durability, before it can be reliably used for the proposed applications. The RSMs developed in this study are based on the proportions of pH-adjusted FG, FA, and PC used in any given composition and represent useful tools for practical comparison and selection of different compositions. However, a new set of

RSMs based on the proportion of different hydration products within the hardened material could also be developed to provide a mechanistic prediction of the performance of any given composition.

Future research should also focus on: (1) improving the strength and durability of this material, e.g., by reducing the variability introduced by inhomogeneous addition of alkali material and prolonged weather exposure; and (2) investigating the use of appropriately modified FG-based blends as cementitious materials used to build reinforced concrete structures. For this different application, a completely new set of properties (e.g., corrosivity for steel reinforcement bars and resistance to freeze-thaw cycles) should also be investigated.

Conflict of interest

None.

Acknowledgements

Support of this research by the Louisiana Department of Wildlife and Fisheries through award #724534 is gratefully acknowledged. Brown Industries, Big Cajun II Power Plant, and Buzzi Unicem USA are also gratefully acknowledged for donating the materials used in this research. Any opinions, findings, conclusions, or recommendations expressed in this publication are those of the writers and do not necessarily reflect the views of the sponsoring agencies.

References

[1] UNEP, Solid Waste Management, United Nations Environment Programme, CalRecovery, Concord, CA, USA, 2005.
[2] W. Halstead, Potential for Utilizing Industrial Wastes and By-Products in Construction of Transportation Facilities in Virginia, FHWA/VA-80/15, National Technical Information Service, Alexandria, VA, USA, 1979.
[3] J.R. Clifton, P.W. Brown, G. Frohnsdorff, Uses of waste materials and by-products in construction. Part I, Resour. Recovery Conserv. 5 (2) (1980) 139–160.
[4] J.R. Clifton, P.W. Brown, G. Frohnsdorff, Uses of waste materials and by-products in construction. Part II, Resour. Recovery Conserv. 5 (3) (1980) 217–228.
[5] ACAA., Beneficial use of coal combustion products, American Coal Ash Association, Farmington Hills, MI, USA. <https://www.acaa-usa.org/Portals/9/Files/PDFs/Production-and-Use-Brochure.pdf>/, 2014 (accessed on Nov. 20, 2016).
[6] E. Worrell, L. Price, N. Martin, C. Hendriks, L.O. Meida, Carbon dioxide emissions from the global cement industry, Ann. Rev. Energy Environ. 26 (1) (2001) 303–329.
[7] S. Perry, J. Klemeš, I. Bulatov, Integrating waste and renewable energy to reduce the carbon footprint of locally integrated energy sectors, Energy 33 (10) (2008) 1489–1497.
[8] K.S. Sajwan, A.K. Alva, T. Punshon, I. Twardowska, Coal Combustion Byproducts and Environmental Issues, Springer, New York, NY, USA, 2006.
[9] R. Taha, R. Seals, M. Tittlebaum, D. Saylak, Environmental characteristics of by-product gypsum, Transp. Res. Rec. 1486 (1995) 21–26.
[10] W.H. Chesner, R.J. Collins, M.H. MacKay, User Guidelines for Waste and By-Product Materials in Pavement Construction, FHWA-RD-97-148, Rept. No. 480017, Turner-Fairbank Highway Research Center, McLean, VA, USA, 1998.
[11] USGS, Mineral Commodity Summary. Fluorspar, US Geological Survey, Reston, VA, USA. <http://minerals.usgs.gov/minerals/pubs/commodity/fluorspar/280499.pdf>/, 2002 (accessed on Oct. 16, 2016).
[12] J. Aigueperse, P. Mollard, D. Devilliers, M. Chemla, R. Faron, R. Romano, J.P. Cuer, Fluorine Compounds, Inorganic, Ullmann's Encyclopedia of Industrial Chemistry, Wiley-VCH Verlag GmbH & Co. KGaA, Weinheim, Germany, 2000. doi: 10.1002/14356007.a11-307.
[13] T. Lind, Ash Formation in Circulating Fluidized Bed Combustion of Coal and Solid Biomass Ph.D. Dissertation, Technical Research Centre of Finland, Espoo, Finland, 1999.
[14] R.H. Brink, Use of waste sulfate on transpo'72 parking lot. Proc., Third International Ash Utilization Symposium. Sponsored by National Coal Association, Edison Electric Institute, American Public Power Association, National Ash Association, and Bureau of Mines, Pittsburgh, PA, USA, 1973.
[15] M.A. Usmen, L.K. Moulton, Construction and performance of experimental base course test sections built with waste sulfate, lime, and fly ash, Transp. Res. Rec. 998 (1984) 52–62.
[16] Z. Zhang, M. Tao, Stability of Calcium Sulfate Base Course in a Wet Environment, FHWA/LA.06/419, Louisiana Transportation Research Center, Baton Rouge, LA, USA, 2006.
[17] M. Singh, M. Garg, Activation of fluorogypsum for building materials, J. Sci. Ind. Res. 68 (2) (2009) 130.
[18] P. Coquard, R. Boistelle, Water and solvent effects on the strength of set plaster, Int. J. Rock Mech. Min. Sci. Geomech. Abstr. 31 (5) (1994) 517–524.
[19] Y. Bigdeli, M. Barbato, M.T. Gutierrez-Wing, C.D. Lofton, Use of slurry fluorogypsum (FG) with controlled pH-adjustment in FG-based blends, Constr. Build. Mater. 163 (2018) 160–168.
[20] C.D. Lofton, M. Barbato, Y. Bigdeli, J. Jung, J. Jang, K.A. Rusch, M.T. Gutierrez-Wing, Estimating sulfate effective diffusion coefficients of stabilized fluorogypsum for aquatic applications. J. Environ. Eng., ASCE, 2018 (In press), DOI: 10.1061/(ASCE)EE.1943-7870.0001419.
[21] E. Nawy, Reinforced Concrete: A Fundamental Approach, 4th Edition., Prentice Hall, Upper Saddle River, NJ, USA, 2000.
[22] K.A. Rusch, R.K. Seals, T. Guo, Development of Economically Stabilized Phosphogypsum Composites for Saltwater Application. FIPR Project No. 99-01-162R, Louisiana State University, Baton Rouge, LA, USA, 2001.
[23] K.A. Rusch, R.K. Seals, T. Guo, Development of Economically Stabilized Phosphogypsum Composites for Saltwater Application, FIPR Project No. 99-01-162S, Louisiana State University, Baton Rouge, LA, USA, 2005.
[24] Y. Bigdeli, M. Barbato, Use of a low-cost concrete-like fluorogypsum-based blend for applications in underwater and coastal protection structures. Proceedings, Oceans 17, Anchorage, AL, USA, 18-21 September, 2017.
[25] P.K. Mehta, Mechanism of expansion associated with ettringite formation, Cem. Concr. Res. 3 (1) (1973) 1–6.
[26] S. Nagataki, H. Gomi, Expansive admixtures (mainly ettringite), Cem. Concr. Comp. 20 (2) (1998) 163–170.
[27] R.A. Young, The Rietveld Method ISBN 0-19-855577-6, Oxford, United Kingdom, University Press, Oxford, 1993.
[28] ASTM D2216-10 Standard test methods for laboratory determination of water (moisture) content of soil and rock by mass. ASTM International, West Conshohocken, PA, USA, 2010. DOI: 10.1520/D2216-10.
[29] ASTM C192/C192M-16a Standard practice for making and curing concrete test specimens in the laboratory. ASTM International, West Conshohocken, PA, USA, 2016. DOI: 10.1520/C0192-C0192M-16A.
[30] J.A. Cornell, Experiments with Mixtures: Designs, Models, and the Analysis of Mixture Data, 3rd Edition., John Wiley & Sons, New York, NY, USA, 2002.
[31] ASTM D6913-04 (Reapproved 2009), Standard test method for particle-size distribution (gradation) of soils using sieve analysis ASTM International, West Conshohocken, PA, USA, 2009. 10.1520/D6913-04R09.
[32] ASTM D4972-13 Standard test method for pH of soils. ASTM International, West Conshohocken, PA, USA, 2013. DOI: 10.1520/D4972-13.
[33] ASTM C39/C39M-16b Standard test method for compressive strength of cylindrical concrete specimens. ASTM International, West Conshohocken, PA, USA, 2016. DOI: 10.1520/C0039-C0039M-16B.
[34] ASTM C1005-17 Standard test method for reference masses and devices for determining mass and volume for use in the physical testing of hydraulic cements. ASTM International, West Conshohocken, PA, USA, 2017. DOI: 10.1520/C1005-17.
[35] ASTM C806-12 Standard test method for restrained expansion of expansive cement mortar. ASTM International, West Conshohocken, PA, USA, 2017. DOI: 10.1520/C0806-12.
[36] ASTM C878 Standard test method for restrained expansion of shrinkage-compensating concrete. ASTM International, West Conshohocken, PA, USA, 2017. DOI: 10.1520/C0878-C0878M-14A.
[37] L.S. Barcelo, S. Boivin, S. Rigaud, P. Acker, B. Clavaud, C. Boulay, Linear vs. volumetric autogenous shrinkage measurement: material behaviour or experimental artefact. Persson, B., & Fagerlund, G. (Eds.). Self-desiccation and its importance in concrete technology: Proceedings of the second international research seminar in Lund, June 18, 1999. (Report TVBM 3085). Division of Building Materials, LTH, Lund University, Lund, Sweden, 1999.
[38] P. Lura, M.J. Ole, Measuring techniques for autogenous strain of cement paste, Mater. Struct. 40 (4) (2007) 431–440.
[39] Z. Hu, C. Shi, Z. Cao, Z. Ou, D. Wang, Z. Wu, L. He, A review on testing methods for autogenous shrinkage measurement of cement-based materials, J. Sustainable Cem. -Based Mater. 2 (2) (2013) 161–171.
[40] M. Garg, A. Pundir, Investigation of properties of fluorogypsum-slag composite binders–hydration, strength and microstructure, Cem. Concr. Composites 45 (2014) 227–233.
[41] MathWorks, Curve Fitting Toolbox: User's Guide, MathWorks, Natick, MA, USA. < http://cda.psych.uiuc.edu/matlab_pdf/curvefit.pdf >/, 2004 (accessed on Oct. 19, 2016).
[42] K.E. Atkinson, An Introduction to Numerical Analysis, John Wiley, New York, USA, 1978.
[43] C. Runge, Über empirische Funktionen und die Interpolation zwischen äquidistanten Ordinaten, Zeitschrift für Mathematik und Physik (in German) 46 (20) (1901) 224–243.
[44] USACE, Coastal Engineering Manual (CEM), Engineer Manual 1110-2-1100, U. S. Army Corps of Engineers, Washington, DC, USA, 2002.
[45] J. Van Der Meer, S. Sigurdarson, Geometrical design of berm breakwaters, Coastal Eng. Proc. 1 (34) (2014) 25.
[46] T. Campbell, L. Benedet, G. Thomson, Design considerations for barrier island nourishments and coastal structures for coastal restoration in Louisiana, J. Coastal Res., SI 44 (2005) 186–202.

[47] K.R. Parker, Field and Numerical Investigation of Wave Power and Shoreline Retreat in Terrebonne Bay, Southern Louisiana. MS Thesis, Louisiana State University and Agricultural and Mechanical College, Baton Rouge, LA, USA, 2014.
[48] ASTM C469/C469M-14 Standard test method for static modulus of elasticity and Poisson's ratio of concrete in compression. ASTM International, West Conshohocken, PA, USA, 2014. DOI: 10.1520/C0469-C0469M-14.
[49] ASTM C403/C403M-08 Standard test method for time of setting of concrete mixtures by penetration resistance. ASTM International, West Conshohocken, PA, USA, 2008. DOI: 10.1520/C0403-C0403M-08.
[50] ASTM C1754/C1754M-12 Standard test method for density and void content of hardened pervious concrete. ASTM International, West Conshohocken, PA, USA, 2012. DOI: 10.1520/ C1754-C1754M-12.
[51] ASTM C29/C29M-16 Standard test method for bulk density (unit weight) and voids in aggregate. ASTM International, West Conshohocken, PA, USA, 2016. DOI: 10.1520/C0029_C0029M-16.
[52] J. Colombani, J. Bert, Holographic interferometry study of the dissolution and diffusion of gypsum, Water Geochimica et Cosmochimica Acta 71 (8) (2007) 1913–1920.
[53] M.R. Christoffersen, The kinetics of dissolution of calcium sulphate dehydrate in water, J. Cryst. Growth 35 (1) (1976) 79–88.
[54] P.K. Mehta, J.M. Monteiro, Concrete, Structure, Properties and Materials, 4th Edition., McGraw-Hill Education, New York City, NY, USA, 2013.
[55] T.C. Hansen, Recycling of Demolished Concrete and Masonry, Taylor and Francis Group, New York City, NY, USA, 2004.
[56] R. Fikes, Artificial Reefs of the Gulf of Mexico: A Review of Gulf State Programs & Key Considerations, National Wildlife Federation, Merrifield, VA, USA, 2013.